

STRANGE CONTENT OF THE NUCLEON (NuTeV)

T. ADAMS^{4,*}, A. ALTON⁴, S. AVVAKUMOV⁷, L. de BARBARO⁵,
 P. de BARBARO⁷, R. H. BERNSTEIN³, A. BODEK⁷, T. BOLTON⁴, J. BRAU⁶,
 D. BUCHHOLZ⁵, H. BUDD⁷, L. BUGEL³, J. CONRAD², R. B. DRUCKER⁶,
 R. FREY⁶, J. FORMAGGIO², J. GOLDMAN⁴, M. GONCHAROV⁴,
 D. A. HARRIS⁷, R. A. JOHNSON¹, S. KOUTSOLIOTAS², J. H. KIM²,
 M. J. LAMM³, W. MARSH³, D. MASON⁶, C. MCNULTY², K. S. MCFARLAND⁷,
 D. NAPLES⁴, P. NIENABER³, A. ROMOSAN², W. K. SAKUMOTO⁷,
 H. SCHELLMAN⁵, M. H. SHAEVITZ², P. SPENTZOURIS², E. G. STERN²,
 B. TAMMINGA², M. VAKILI¹, A. VAITAITIS², V. WU¹, U. K. YANG⁷, J. YU³
 and G. P. ZELLER⁵

**Presented by T. ADAMS*

¹*University of Cincinnati, Cincinnati, OH, USA*

²*Columbia University, New York, NY, USA*

³*Fermi National Accelerator Laboratory, Batavia, IL, USA*

⁴*Kansas State University, Manhattan, KS, USA*

⁵*Northwestern University, Evanston, IL, USA*

⁶*University of Oregon, Eugene, OR, USA*

⁷*University of Rochester, Rochester, NY, USA*

The NuTeV experiment uses neutrino deep-inelastic scattering from separate neutrino and anti-neutrino beams to study the structure of the nucleon. Charged-current production of charm is sensitive to the strange content of the nucleon while neutral-current charm production probes the charm content. Preliminary analyses of both topics are presented along with discussion of possible momentum asymmetry in the strange sea.

Charm production is a significant fraction of the total neutrino deep-inelastic scattering (DIS) cross-section. The semi-muonic decay of charm mesons creates unique final states with which to study exclusive charm production. For charged-current reactions, an opposite-signed two muon (dimuon) final state is possible. Neutral-current production can create an event with a single muon with charge opposite that which is expected from a charged-current interaction (wrong-signed muon). Feynman diagrams for both reactions are shown in Fig. 1.

The NuTeV experiment studies ν and $\bar{\nu}$ DIS using the Sign-Selected Quadrupole Train (SSQT) beam and the Fermilab Lab E detector.¹ The SSQT allows separate running of neutrino and anti-neutrino beams. The (anti-)neutrino beam is incident upon the Lab E target/calorimeter. The target/calorimeter has 42 segments each consisting of two liquid-scintillator counters and one drift chamber interspersed in 20 cm of iron. The calorimeter provides energy

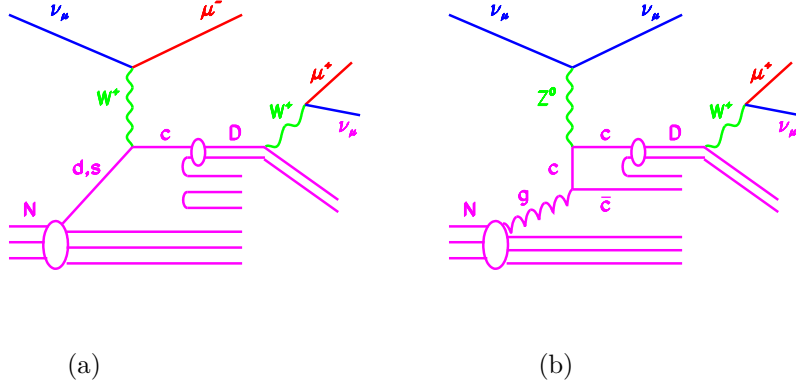


Figure 1: Feynman diagrams for (a) charged-current and (b) neutral-current charm production via neutrino DIS.

and position measurement for hadronic/electromagnetic showers and a position measurement for deeply-penetrating muon tracks. Immediately downstream of the calorimeter is a toroid spectrometer which provides momentum and charge measurement for the muons entering it. The NuTeV analyses presented here use the full data sample from the Fermilab 1996-97 fixed target run.

1 Charged-Current Charm Production

Neutrino charged-current DIS charm production results from scattering off d or s quarks in the nucleon. The Cabibbo suppression of scattering off d quarks greatly enhances the contribution of the s quarks. This allows the strange content of the nucleon to be probed.

The dimuon data set consists of events passing fiducial and kinematic selections and containing a hadronic shower (> 10 GeV) with at least two muons. One muon must be toroid analyzed with more than 9 GeV in energy while the other muon must have more than 5 GeV in energy. The two sources of such events are charged-current charm production and a charged-current event with a π/K decaying within the shower. Both sources are included within the dimuon Monte Carlo simulation.

Data and Monte Carlo are binned in three variables:

$$x_{vis} = \frac{E_{vis} E_{\mu 1} \theta_{\mu 1}^2}{2m_p (E_{\mu 2} + E_{had})} \quad (1)$$

$$E_{vis} = E_{\mu 1} + E_{\mu 2} + E_{had} \quad (2)$$

$$z_{vis} = \frac{E_{\mu 2}}{E_{\mu 2} + E_{had}} \quad (3)$$

where the subscript *vis* (*visible*) refers to measured variables, $\mu 1$ is the primary muon (from the primary vertex) and $\mu 2$ is the secondary muon (from the decay vertex). The Monte Carlo is weighted by the leading-order (LO) cross-section and normalized to agree with the two-muon data.

Four parameters are used to describe charged-current charm production. κ determines the size of the strange sea relative to the non-strange sea ($\kappa \sim \frac{2\bar{s}}{\bar{u}+\bar{d}}$). The shape of the strange sea is described by $(1-x)^\beta$. m_c is the mass of the charm quark and ϵ determines the Collins-Spiller fragmentation.² These parameters are varied to find the best agreement between data and Monte Carlo.

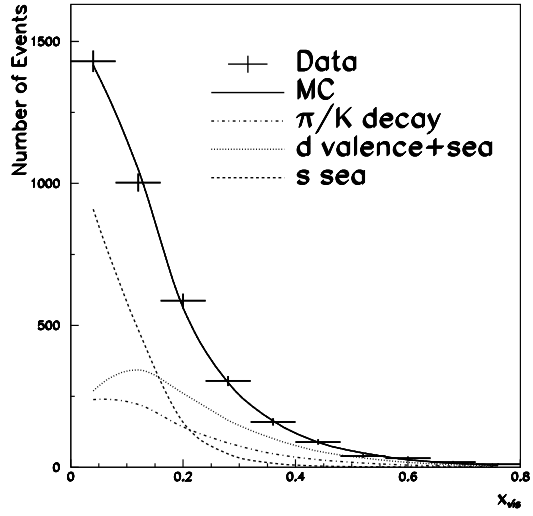
Figures 2 and 3 show comparisons of data and Monte Carlo after fitting. The distributions of x_{vis} are shown in Fig. 2 with a breakdown of the components of the simulation. The dominance of production off the strange sea can be clearly seen. There is excellent agreement for various other distributions which have been compared, some of which are shown in Fig 3.

The preliminary results of the fit are:

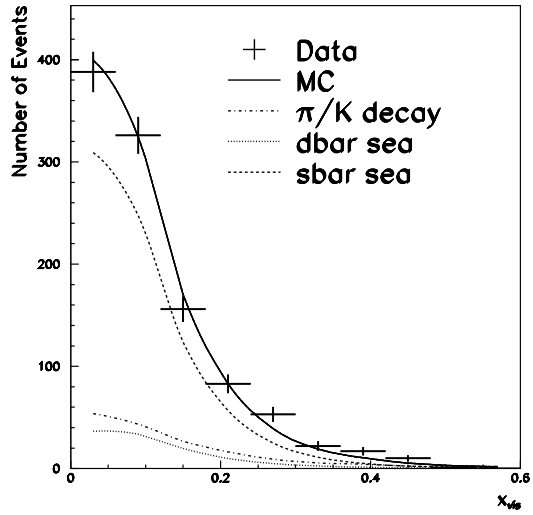
$$\begin{aligned} \kappa &= 0.42 \pm 0.07 \pm 0.06 \\ \beta &= 8.5 \pm 0.56 \pm 0.39 \quad (\text{at } Q^2 = 16 \text{ GeV}^2) \\ m_c &= 1.24 \pm 0.25 \pm 0.46 \text{ GeV} \\ \epsilon &= 0.93 \pm 0.11 \pm 0.15 \end{aligned}$$

where the first error is statistical and the second error is systematic. The contributions to the systematic error are shown in Table 1. The largest systematic error is from the (anti-)neutrino flux which is expected to be reduced by further work. However, the errors for κ and α are already statistics limited so the improvement will be primarily for m_c and ϵ .

The results of this analysis for the strange sea compare favorably with previous measurements. CHARM II,³ CCFR⁴ and CDHS⁵ have all measured the size of the strange sea to be $\sim 40\%$ of the non-strange sea. The value of β is consistent with CCFR's analysis which used the same form for the momentum distribution. Figure 4 shows a comparison of the results of the CCFR and NuTeV strange sea measurements. There is excellent agreement between the two measurements. Figure 5 compares the NuTeV result to theoretical predictions from CTEQ and GRV. The NuTeV result is lower than the CTEQ prediction while in better agreement with GRV.



(a)



(b)

Figure 2: Comparison of the NuTeV data with results of the fit for the variable x_{vis} in both ν (a) and $\bar{\nu}$ (b) mode.

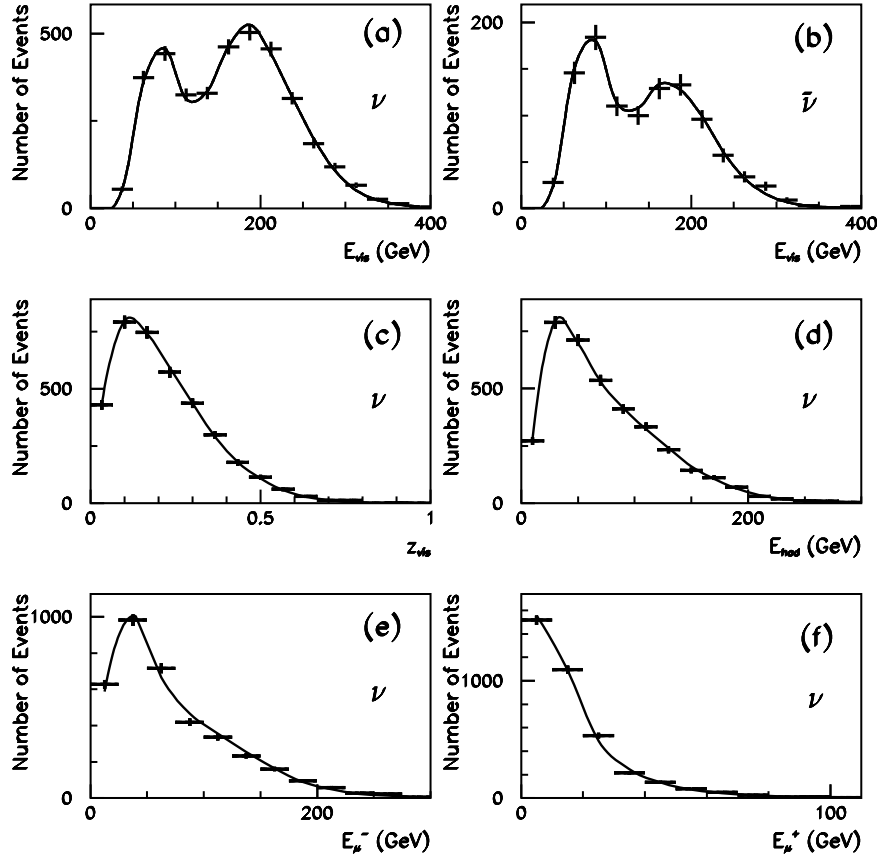


Figure 3: Comparison of the NuTeV data with results of the fit for several variables: E_{vis} (ν mode) (a); E_{vis} ($\bar{\nu}$ mode) (b); z_{vis} (ν mode) (c); E_{HAD} (ν mode) (d); E_{μ^-} (ν mode) (e); E_{μ^+} (ν mode) (f);

Table 1: Systematic errors for the parameters of the CC charm production analysis.

	κ	β	m_c	ϵ
Hadron Calibration (1%)	0.03	0.09	0.06	0.06
Muon Calibration (1%)	0.02	0.14	0.11	0.05
Monte Carlo Calibration	0.00	0.003	0.02	0.02
R_L (20%)	0.00	0.10	0.03	0.01
π/K decay (ν 15% $\bar{\nu}$ 21%)	0.02	0.17	0.01	0.08
Charm quark semi-muonic BF (10%)	0.01	0.004	0.01	0.05
Monte Carlo Statistics	0.02	0.11	0.05	0.02
Flux	0.03	0.28	0.44	0.08
Total Systematic	0.06	0.40	0.46	0.15
Statistics	0.07	0.56	0.25	0.11

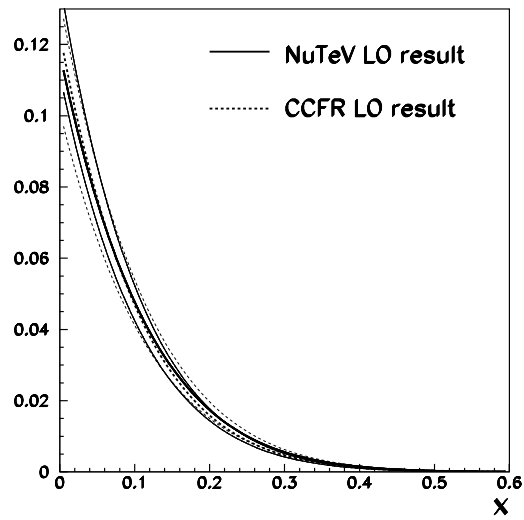


Figure 4: Comparison of the NuTeV (with error bands) result to the CCFR result.

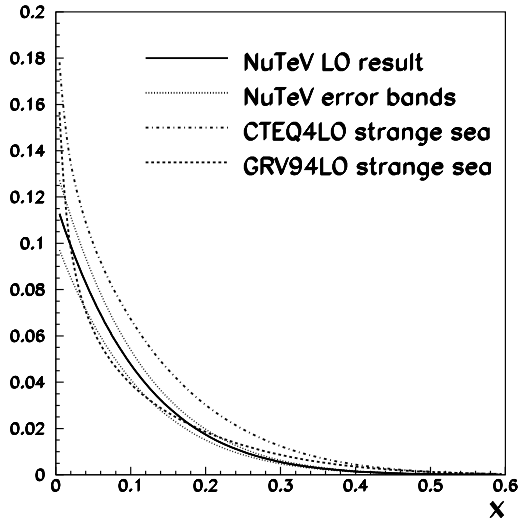


Figure 5: Comparison of the NuTeV (with error bands) result to theoretical predictions from CTEQ and GRV.

2 Asymmetric Strange Sea

Predictions have been made that the nucleon strange sea may have an asymmetry between the s and \bar{s} momentum distributions.⁶ If the nucleon has a sizeable s contribution at moderate x it is possible for the nucleon wavefunction to contain intrinsic s states such as $K^+\Lambda$. The Brodsky and Ma model⁶ predicts the s momentum distribution will be harder than the \bar{s} distribution.

The CCFR collaboration has performed a test of this hypothesis. The s and \bar{s} momentum distributions were allowed to have different shapes ($(1-x)^\beta$ and $(1-x)^{\beta'}$) while the total contributions were constrained to be equal:

$$\int_0^1 s(x)dx = \int_0^1 \bar{s}(x)dx. \quad (4)$$

The fit to the CCFR data yielded a shape difference, $\Delta\beta = \beta - \beta'$, of $-0.46 \pm 0.42 \pm 0.76$. This indicates the s and \bar{s} momentum distribution are consistent. A 90% limit can be set on the difference:

$$-1.9 < \Delta\beta < 1.0 \quad (5)$$

The strange sea asymmetry is currently being explored by the NuTeV collaboration.

3 Neutral-Current Charm Production

Neutral-current (NC) charm production occurs via scattering off charm quarks in the nucleon (Fig. 1(b)). Analysis of this reaction probes the charm content of the nucleon. While some models allow for an intrinsic charm content of the nucleon, this analysis only considers gluon splitting as its source for charm.

This analysis considers events which have a single muon with the opposite charge from charged-current interactions of the selected beam type (wrong-sign events). This is possible because of NuTeV's low contamination of wrong type neutrinos in the beam and the ability to select the beam type (ν or $\bar{\nu}$).

There are three sources of wrong-sign events other than NC charm production. The largest source is from charged-current interactions initiated by wrong type neutrinos in the beam. This contamination is less than 2×10^{-3} of the beam intensity. Also included in this category are charged-current events where the sign of the muon is mis-identified (generally due to a large scatter in the toroid spectrometer). The second largest source comes from two-muon events (see Section 1) where the primary muon is not measured because it is of low energy or exits the detector. The third source comes from NC events where a π/K in the shower decays prior to interacting.

Figure 6 shows the wrong-sign muon data from NuTeV (points) for the variable $y_{vis} = \frac{E_{HAD}}{E_{HAD} + E_{\mu}}$. The predictions for the individual background sources and their sum are also shown. A clear excess of events is seen at high y_{vis} . Figure 7 shows predictions for neutral-current charm production which peaks in the same region as the excess.⁷

4 Summary

The NuTeV sign-selected neutrino beams allow for improved studies of the strange and charm contributions to the nucleon sea. The strange sea is observed to be in agreement with previous measurements with a size which is $0.42 \pm 0.07 \pm 0.06$ the size of the average non-strange sea and a shape $(1-x)^{8.5 \pm 0.56 \pm 0.39}$ (at $Q^2 = 16 \text{ GeV}^2$). CCFR found no evidence for an asymmetric strange sea; NuTeV is still investigating the subject. The wrong-sign muon data shows a clear excess of events which is consistent with neutral-current charm production.

Acknowledgments

We gratefully acknowledge the substantial contributions of the staff of the Fermilab Beams and Particle Physics Divisions to the construction and operation of the NuTeV beamlines and the Lab E detector. This work was sponsored in

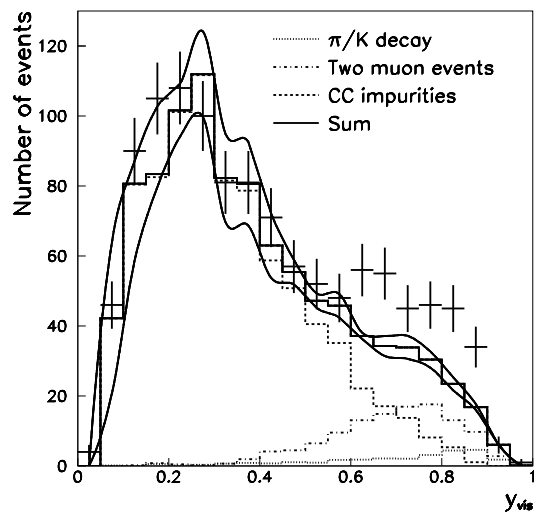


Figure 6: NuTeV wrong-sign muon data (points) compared to the sum of the background sources (solid histogram) and systematic errors (curve). The individual background components are also shown as histograms.

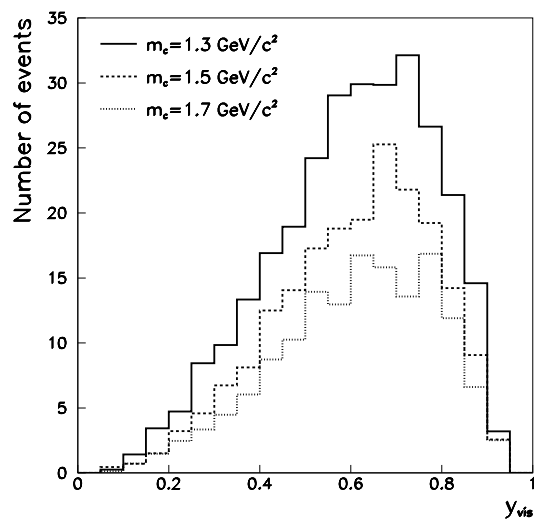


Figure 7: Predictions of neutral-current charm production for various values of $m_c = 1.3, 1.5, 1.7$ (ν mode only).

part by funding from the U.S. Department of Energy and the National Science Foundation.

References

1. Sakumoto, W.S., *et al.*, *Nucl. Instrum. Methods.* **A 294**, 179 (1991);
King, B.J., *et al.*, *Nucl. Instrum. Methods.* **A 302** 254 (1991).
2. Collins, P. and Spiller, T., *J. Phys.* **G 11**, 1289 (1985).
3. Vilain, P., *et al.*, *CERN-EP/98-128* (1998).
4. Rabinowitz, S.A., *et al.*, *Phys. Rev. Lett.* **70**, 134 (1993).
5. Abramowitz, H., *et al.*, *Z. Phys.*, **C 15**, 19 (1982).
6. Brodsky, S. and Ma, B., *Phys Lett.*, **B381**, 317 (1996).
7. Gluck, M., *et al.*, *Z. Phys.*, **C 38**, 441 (1988).